

Received: 2020.07.08

Accepted: 2020.08.25

Available online: 2020.09.23

Published: 2020.11.16

Construction of a *Mex3c* Gene-Deficient Mouse Model to Study C-FOS Expression in Hypothalamic Nuclei and Observe Morphological Differences in Embryonic Neural Tube Development

Authors' Contribution:

Study Design A

Data Collection B

Statistical Analysis C

Data Interpretation D

Manuscript Preparation E

Literature Search F

Funds Collection G

ABDE 1,2 Yong Du*
BCEF 3 Quan Huo*
BCD 3 Ting Li
BEF 3 Dongjun Sun
BCD 4 Ting Sun
BEF 3 Zhiguo Lu

1 Department of Laboratory Surgery, General Hospital of Ningxia Medical University, Yinchuan, Ningxia, P.R. China
2 Department of Pediatric Surgery, General Hospital of Ningxia Medical University, Yinchuan, Ningxia, P.R. China
3 Department of Pediatric Surgery, College of Clinical Medicine, Ningxia Medical University, Yinchuan, Ningxia, P.R. China
4 Biological Sample Bank, General Hospital of Ningxia Medical University, Yinchuan, Ningxia, P.R. China

* Yong Du and Quan Huo contributed equally

Corresponding Author: Yong Du, e-mail: dyningxia@163.com

Source of support: This work was supported by a grant from the National Natural Science Foundation of China (No. 81560253)

Background: This study utilized CRISPR/Cas9 gene editing technology to construct a *Mex3c* gene-deficient mouse model, and studied C-FOS expression in hypothalamic nuclei.


Material/Methods: Thirty *Mex3c*^{-/-} mice, 30 mice in the normal group, and 30 *Mex3c*^{-/+} mice were randomly divided into control, leptin, and ghrelin groups according to different intraperitoneal injections. HE and Nissl staining were performed to observe the morphology of hypothalamic nerve cells. The C-FOS expression in hypothalamic nuclei of each group was analyzed by immunohistochemical techniques. HE staining was used to observe neural tube morphology, and LFB staining was used to observe nerve myelin sheath morphology. TEM was used to observe neuronal ultrastructure and immunohistochemical techniques were utilized to analyze nestin expression.

Results: C-FOS expression was lower in the normal control group than in the leptin and ghrelin groups. The *Mex3c* control group and the leptin group had higher C-FOS expression than the ghrelin group. In neural tube studies, no significant differences were found in the neural tube pathological sections of E14.5-day embryos in each group. Nestin results demonstrated lower expression in the normal group and there was little difference between the HD and *Mex3c* groups.

Conclusions: *Mex3c* appears to participate in the regulation of energy metabolism by inducing C-FOS expression in the hypothalamus. The neural tubes of the offspring of *Mex3c*^{-/+} mice had defects during development.

MeSH Keywords: **Clustered Regularly Interspaced Short Palindromic Repeats • Energy Metabolism • Hypothalamus • Neural Tube**

Full-text PDF: <https://www.medscimonit.com/abstract/index/idArt/927334>

 3346

 2

 5

 28



Background

CRISPR (clustered regularly interspaced short palindromic repeats) and CRISPR-associated endonuclease Cas is a genetic editing technology that has emerged in recent years, called CRISPR/Cas9 [1]. The acquisition time of mutant mice and rats can be significantly shortened, from 1 year to several weeks, which satisfies the needs of investigators for rapid and effective editing of organism genome, modifying cations, and the construction of specific gene knockout animal models [2,3]. Through this approach, we obtained Mex3c gene-deficient mice that meet the experimental demands.

The energy balance depends upon the balance between food intake regulation and energy expenditure. The hypothalamic nucleus of the paraventricular nucleus (PVN), arcuate nucleus (Arc), medial nucleus (DMN), ventromedial nucleus (VMN), and lateral nucleus (LHA) affect appetite, which plays a vital role in energy balance regulation [4]. Since the initial study of *C. elegans* in 1996, Mex3c has been found to be a conserved RNA-binding protein in organisms ranging from nematodes to humans [5]. Related investigations have reported that the Mex3c gene can cause genetically predisposed hypertension, control RNA instability in malignant tumors, and reduce body fat accumulation by promoting energy expenditure [6,7]. Mex3c^{-/-} mice have no significant differences in muscle mass compared to control mice, but it is unclear whether the fat mass decreases are related to decreased leptin expression. Therefore, we designed mouse models expressing the leptin gene and the Mex3c gene heterozygous and homozygous mutations. The results showed that the leptin content in these 2 models could not be detected, which further suggested that the Mex3c mutation is associated with a negative energy balance [8]. As a metabolic marker of neural activity, C-FOS participates in physiological functions such as cell growth, differentiation, and information transmission. After receiving exogenous stimulation, the expression level of the original basal level is significantly increased [9,10]. In studies of energy balance, various signals were found to be involved in energy balance regulation, such as leptin and ghrelin signal transduction, by inducing postsynaptic C-FOS expression [11,12]. To investigate the relationship between Mex3c and C-FOS in neuronal signal transduction, we constructed a Mex3c knockout mouse model. We injected mice with leptin (causing a negative energy balance effect) and ghrelin (causing a positive energy balance effect), which induced neurons expressing C-FOS in a signal pathway involved in energy balance. By examining the C-FOS expression under these stimuli, we provided an anatomical basis for the mechanism through which Mex3c regulates energy balance.

Neural tube defects are common and serious congenital malformations, the etiology of which is complex, and can be caused by biological genetic and environmental factors [13].

The important role of energy metabolism in neural tube closure has been validated in some animal models. For instance, Yamaguchi et al. reported that, during mammalian pregnancy, neural tube defects can be caused by malnutrition and insufficient or excessive intake of specific nutrients [14]. The Mex3c gene has an important role in energy metabolism process in the body. This study aimed to explore the mechanism by which Mex3c regulates energy balance and to assess whether it participates in neural tube formation.

Material and Methods

Construction of the Mex3c gene-deficient mouse model

The Mex3c gene-deficient mouse model was constructed by Cyagen Biosciences (Guangzhou), Inc. Three male and 3 female mice were obtained and raised at the Ningxia Medical University SPF Laboratory Animal Center (12-h light/dark cycle, temperature 22±2°C, humidity 50±5%, with clean feed and water) to breed a sufficient number of experimental mice. The Animal Experimental Ethics Committee of Ningxia Medical University approved this study, and the animal treatment process was in line with animal ethics standards. 30 wild-type (WT) and 30 Mex3c^{-/-} mice (8 weeks old; female) were used. Mice in each group were randomly divided into a control group, a leptin group, and a starvation hormone group. Sodium pentobarbital (1%) was intraperitoneally injected for anesthesia. We opened the chest to expose the heart, cut the left atrium, and rinsed it with 20 mL of normal saline from the right ventricle. After the left ventricle outflow was clear, we performed continuous infusion with 4% paraformaldehyde 10 mL with slow injection over a period of 10 min. The mouse brain was removed after anesthesia and we obtained paraffin-embedded preservation tissue. The WT and Mex3c^{-/-} mice were fed with normal feed and high-sugar and high-fat diets (experimental Animal Premix 2.0%, calcium hydrogen phosphate 2.0%, soy protein isolate 10.0%, lard 12%, sucrose 20%, cholesterol 1.0%, standard mouse maintenance feed 53%; Jiangsu Province Collaborative Medicine Bioengineering Co.). Each group had 10 mice, and the experiment was started at 8 weeks of age. After 12 weeks of continuous feeding, the WT male mice were caged with the female mice at 8:00 pm every day. At 8:00 am the next morning, the female mice were found have the vaginal embolism recorded at 0.5 days of pregnancy. With the feeding conditions unchanged, we anesthetized the females after 14.5 days of pregnancy. The embryos were removed and embedded in paraffin.

Mouse acquisition and genetic identification

When F0 generation mice were 8 weeks of age, males and females were bred to obtain an F1 generation. When the new

Table 1. PCR mixture.

Component	×1
ddH ₂ O	9.5 μl
Product primer F1	1.0 μl
Reverse primer R1	1.0 μl
Premix Taq	12.5 μl
DNA	1.0 μl

female mice were 3 weeks old, after routine disinfection, we cut 3-mm-long tail pieces into 1.5-mL EP tubes and marked them for later use. We added 80 μL of Direct PCR Tail (Viagen Biotech, USA) to each EP tube and kept the tubes in a 55°C water bath overnight. On the next day, 1 μL of proteinase K was added at 80°C for 1 h to extract tissue DNA. We designed specific primers to identify Mex3c gene-deficient mice by PCR. The primer sequences were as follows:

Forward primer F1

5'-GCCACTAGCCATGAACATTATTATC-3';

Forward primer F2

5'-AGGCTGCTATGGT AACACTAACC-3';

Reverse primer R1

5'-CGAGATGAGAGTCAATGTAGCAG-3';

Internal control PCR primer F

5'-CATGCCAATGGTTCACTCTAAGGT-3';

Internal control PCR primer R

5'-TCTCTATGTCCAAAGTGCAGACAC-3'.

The circulation system is listed in Table 1. We configured a 1.5% agarose gel for electrophoresis and the electrophoresis system is shown in Table 2. According to the electrophoresis results, WT mice and Mex3c gene-deficient mice were identified, and they were housed in cages for use in subsequent experiments.

Paraffin embedding of mouse brain and embryo

At 2 h after intraperitoneal injection in the saline group, leptin group, and hunger hormone group, we intraperitoneally injected anesthesia with 1% sodium pentobarbital (0.05 mg/g). After routine disinfection, the heart was opened and the left atrium was cut out and removed. We fully flushed the right atrium with normal saline. After the effluent was clear, we injected 4% paraformaldehyde for about 10 min. We carefully removed the brain tissue and placed it in freshly prepared 4% paraformaldehyde for 1 day. On the next day, we washed the brain tissue with phosphate-buffered saline (PBS), replaced PBS solution every hour 6 times, and then dehydrated with gradient alcohol (alcohol concentration was 70%, 80%, 90%, 95%, 100%, and 100%). We fully infiltrated the tissue with xylene. Paraffin waxes I and II were melted at 65°C and the tissue was immersed in the wax for 2 h for paraffin embedding. At day 14.5 of pregnancy, we routinely performed sterilization and anesthesia and

Table 2. DNA cycling condition.

Step	Temp	Time	Cycles
Initial denaturation	94°C	3 min	
Denaturation	94°C	30 s	
Annealing	52°C	35 s	35×
Extension	72°C	35 s	
Additional extension	72°C	5 min	

found the “Y” type distribution uterus. Afterwards, we carefully separated the gestational sac, and treated the embryo tissue as previously described [1]. We then dehydrated it with gradient alcohol (alcohol concentration 30%, 50%, 70%, 80%, 90%, 95%, 100%, and 100%). Tissue was thoroughly permeated with toluene and immersed in paraffin I and II for 1 h at 65°C as paraffin embedding.

Immunohistochemical staining of mouse hypothalamic nuclear and embryonic neural tubes

Each paraffin-embedded tissue was sectioned with a vibrating slicer (Leica) to a thickness of 4 μm. We used the Mouse Brain Stereotactic Map (second edition, prepared by Keith B. J. Franklin) to locate Arc, VMN, DMN, and PV nuclei of the hypothalamus. We performed conventional dewaxing and hydration and used citrate antigen repair solution for high-pressure repair for 10 min. We used 3% H₂O₂ for removal of endogenous peroxidase, then goat serum blocking and addition of mouse-derived C-FOS primary antibody (1: 300, Proteintech, USA) were performed overnight at 4°C. The tissue was washed with PBS solution according to the rabbit anti-mouse secondary antibody kit instructions (ZSGB-BIO, China). Positive expression was detected by analyzing the percentage of unit area using ImageJ software. We used the nestin (1: 300, Bioss, China) expression to assess the development of the mouse embryonic neural tube. The experimental steps used were similar to those previously described [1].

Electron microscopic observation of ultrastructure

Mouse embryos obtained at 14.5 days of pregnancy were quickly placed in glutaraldehyde for 2 h. We then washed them 3 times in buffer for 2 h. They were processed with osmium tetroxide fixation, then dehydrated, embedded, and sectioned under a Hitachi H-7650 transmission electron microscope (Tokyo, Japan). We observed the development of synapses and mitochondria in mouse embryonic neural tubes.

Statistical analysis

We used SPSS 17.0 statistical software (SPSS, Inc., Chicago, IL, USA) to analyze the experimental data. Measurement data

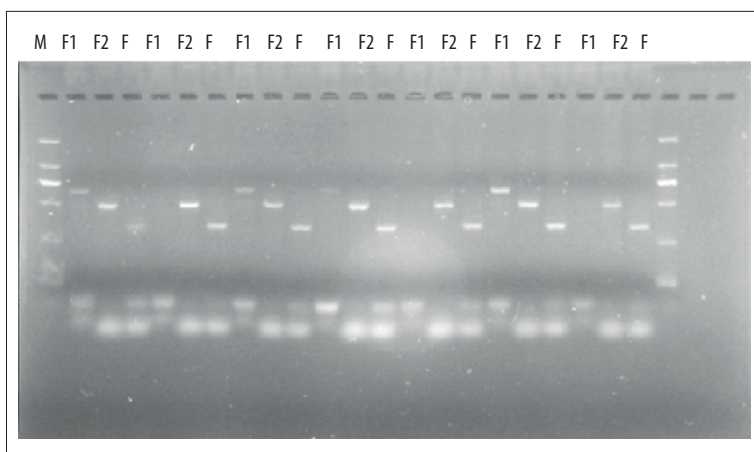


Figure 1. PCR identification of mouse gene gel plate results.

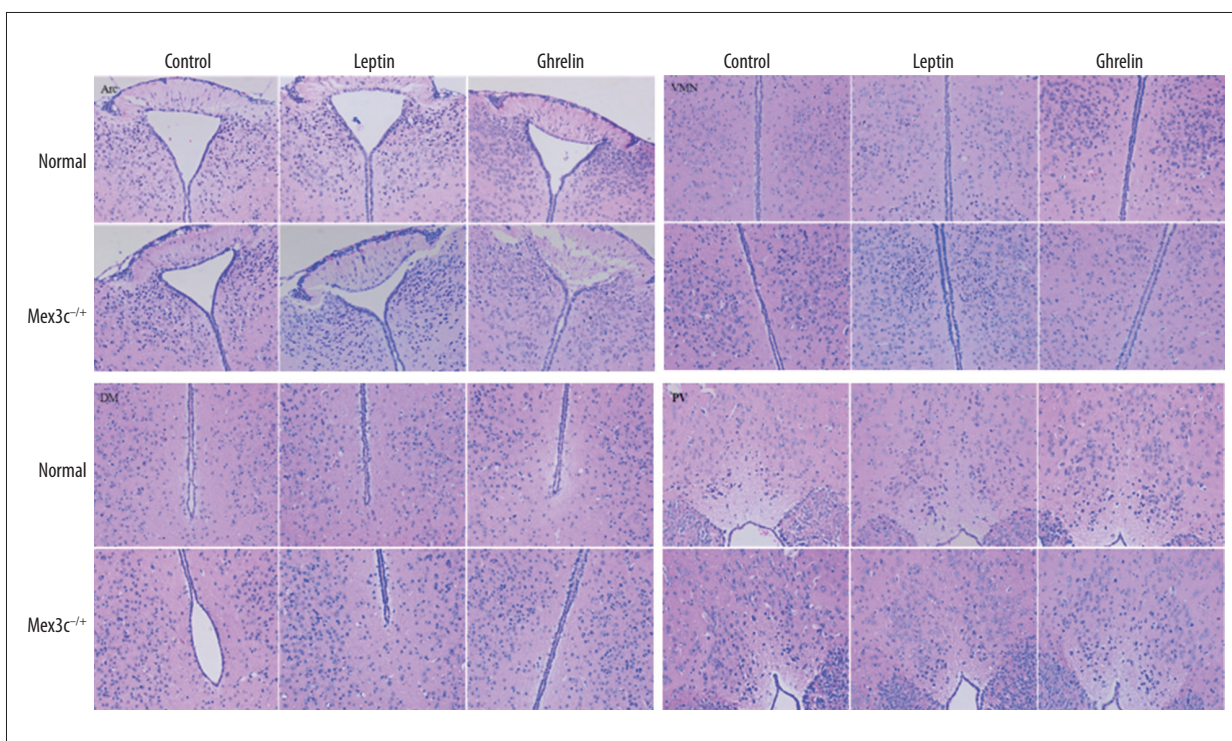


Figure 2. H&E staining results of hypothalamic Arc, VMN, DM, and PV nuclei in each group of mice (x200). Scale bar=100 μm.

are denoted by mean±SEM (X±S). One-way analysis of variance and SNK-q test were utilized for comparison between groups. *P*<0.05 indicated a statistically significant difference.

Results

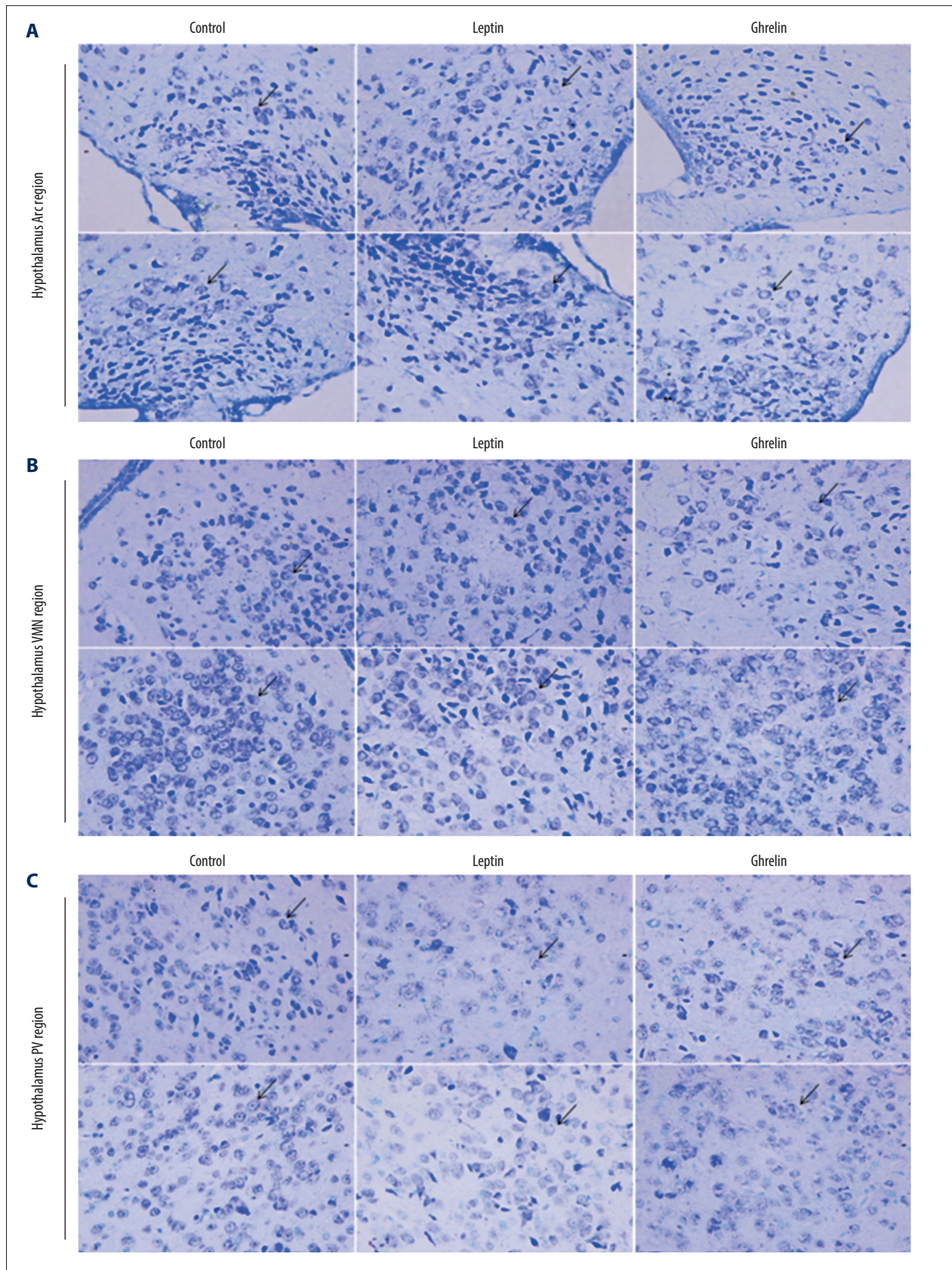
Mex3c^{+/-} mouse genotype identification

The F1 mice obtained by breeding were subjected to Mex3c knockout identification, in which M stands for marker band and 3 consecutive wells represent 1 mouse. F1 primer 640 bp shows a bright band to indicate gene knockout success. F2

primer 499bp-positive means wild-type, combined with F1. The F2-positive result determines pure mouse zygote, heterozygous, wild-type. The F primer 335 bp is the internal reference primer, and both the wild-type and the KO-positive have a strip which ensures that the sample DNA was successfully extracted during the experiment and the PCR was successful. Finally, 30 Mex3c gene-deficient mice were obtained according to the electrophoresis results (Figure 1, PCR results indicated).

Brain histomorphology staining

The hypothalamic partial nuclei of mice were observed by HE staining and Nissl staining technique. HE staining showed that



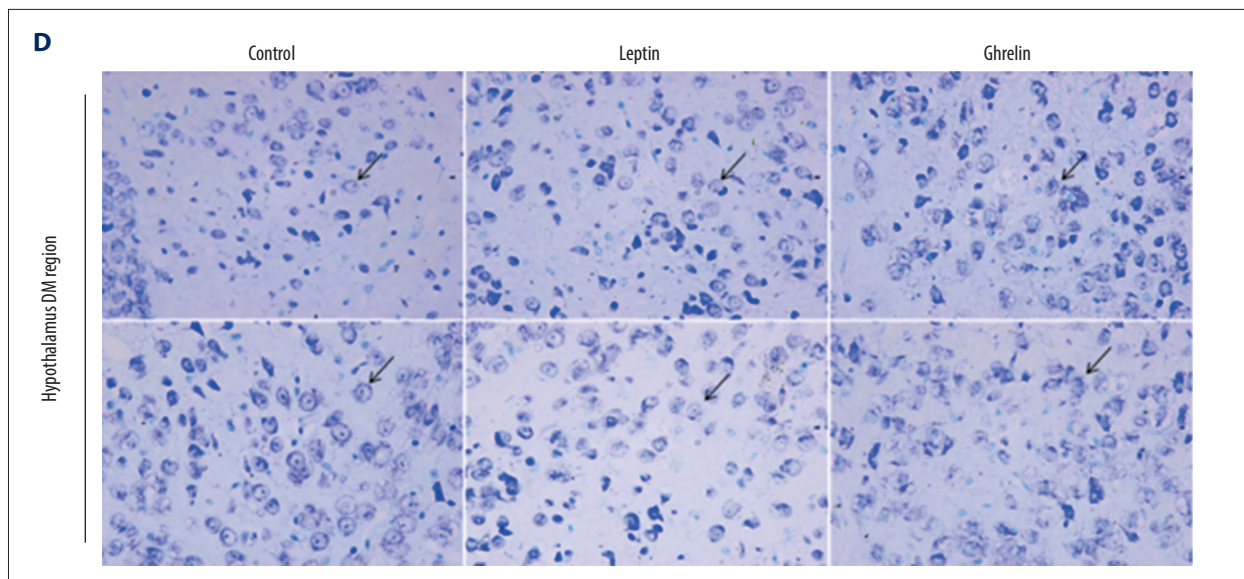


Figure 3. (A) Nissl staining results of hypothalamic Arc nuclei in each group of mice ($\times 400$). (A) Arc nuclei ($\times 400$). (B) VMN nuclei ($\times 400$). (C) DM nuclei ($\times 400$). (D) PV nuclei ($\times 400$). Scale bar=50 μm . Black arrow indicates neuron cells.

the nerve cells in each nucleus were densely packed and densely clustered, with normal morphology and structure of the nucleus tissue. The cytoplasmic staining of the nucleus was dense, with no damage or degeneration, necrotic neurons were observed, and the tissue staining was uniform, anatomical, and clear. Nissl staining showed that the nucleus of the neurons was obviously stained blue, and the cytoplasm was light blue. It can be seen that the Nissl body is evenly distributed in the perinuclear cytoplasm, dyeing is deep or shallow, found in the cytoplasm or in the periphery of the cell, and no staining becomes shallow and blurred. The neuronal cells of each group were large and round and were located in Arc, VMN, DM, and PV nuclei. There was no nuclear dissolution or nuclear pyknosis, and no obvious vacuoles (Figures 2, 3).

C-FOS expression in the hypothalamus

Immunohistochemistry results showed that the 3 intervention treatments of WT mice and Mex3c^{-/-} mice were intraperitoneal injection of normal saline, leptin (causing a negative energy balance effect), and ghrelin (causing a positive energy balance effect). The expression trends of C-FOS in each group were similar in the nuclei of the hypothalamus. We found that expression of C-FOS in the normal control group was very low, but after intervention with leptin and ghrelin, the expression of C-FOS was greatly increased ($p < 0.001$). In the Mex3c^{-/-} mice, the expression of C-FOS was significantly higher in the control group, and the expression of C-FOS was not significantly changed after leptin treatment ($P > 0.05$). However, the expression of C-FOS was significantly decreased after injection of ghrelin compared with the Mex3c^{-/-} control group ($P < 0.001$), and the difference was significant. Finally, we found that the

normal control group and the Mex3c^{-/-} ghrelin group had similar C-FOS expression levels and they had no differences in DM and PV nuclei ($P > 0.05$) (Figure 4).

Morphological differences in neural tube development

We used HE staining, Luxol fast blue (LFB), and immunohistochemical detection to analyze nestin expression in neural tubes. We observed the neural tube ultrastructure by electron microscopy to explore the morphological differences in neural tube development in offspring of the 3 groups of embryonic mice. HE staining showed no significant differences in the morphology of neural tube cells in the control group, Mex3c^{-/-}, and high-sugar and high-fat diet (HD) groups. In the LFB staining results, we observed that myelin sheaths in the control group had a deeper color than those in the other 2 groups. Neural tube transmission electron microscopy (TEM) showed that, compared with the control group, the mitochondrial edema of neuron cells in the neural tube of the embryonic mice of Mex3c^{-/-} and HD groups showed larger numbers of vacuoles. The mitochondrial cristae were broken and the structure was clearly abnormal in the neural tubes of embryonic mice of the Mex3c^{-/-} and HD groups. The presynaptic membrane and postsynaptic membrane were clear but the synaptic space disappeared. The synapses had a certain degree of fusion and the typical structure was difficult to find. We observed that neuronal cells were damaged, and their nuclear chromatin was lost. Also, the nuclei had pyknosis. According to TEM results, Mex3c^{-/-} and HD group mouse embryos had this particular defect during neural tube development. Using immunohistochemical staining technology to detect nestin expression in mouse embryonic neural tubes in each group, we

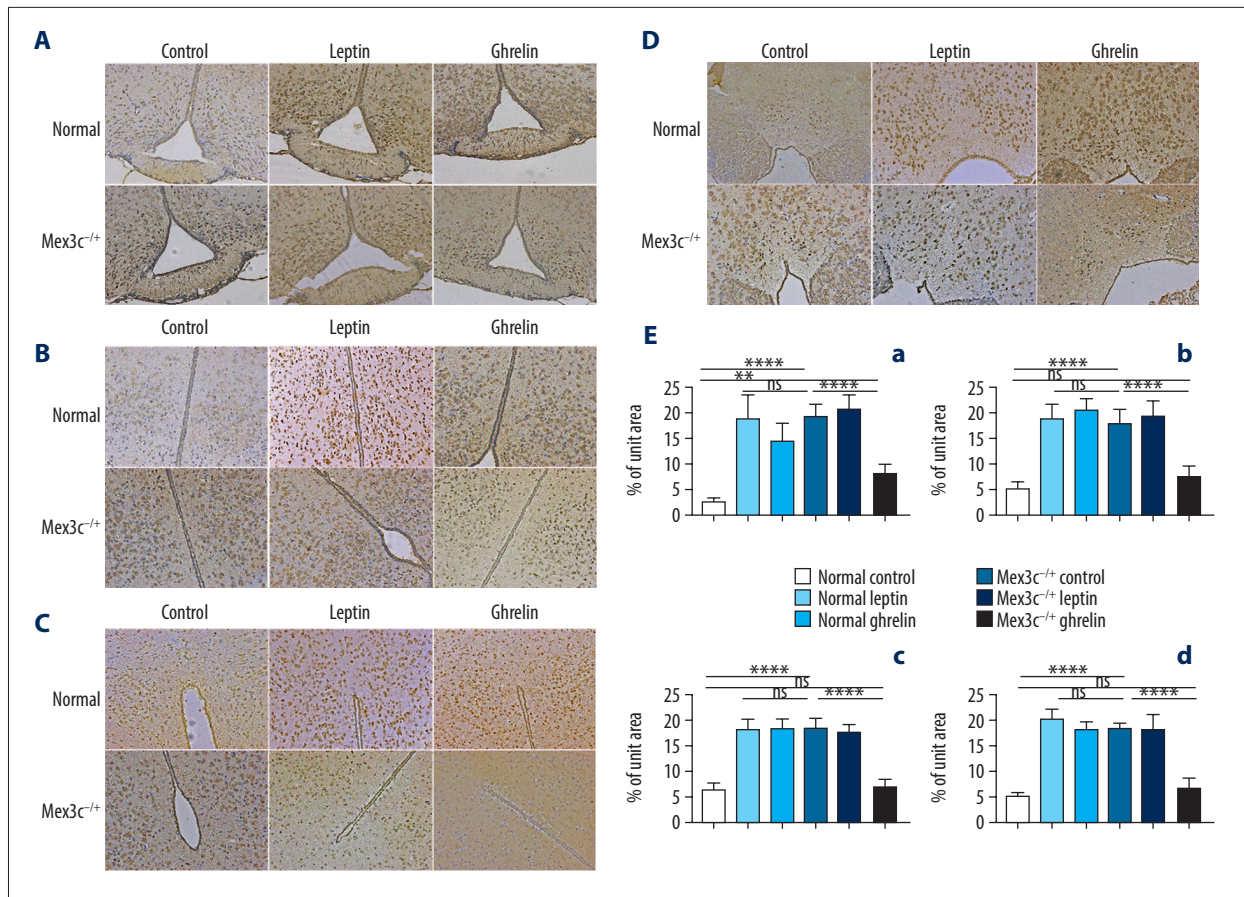


Figure 4. C-FOS expression of hypothalamic nuclei. (A) Arc nuclei ($\times 200$). (B) VMN nuclei ($\times 200$). (C) DM nuclei ($\times 200$). (D) PV nuclei ($\times 200$). Scale bar=100 μ m. (E) The 2 ends of the horizontal line indicate a comparison between the 2 groups. a-d is a bar chart comparing the C-FOS expression levels of the hypothalamic A-D nucleus (* $P < 0.05$, ** $P < 0.01$, **** $P < 0.001$, ns: no significance).

found that the expression of this factor in the Mex3c^{-/-} and HD groups were not significantly different ($P > 0.05$) and its expression was significantly increased compared with the control group ($P < 0.05$) (Figure 5).

Discussion

In this study, we successfully constructed a Mex3c gene-deficient mouse model. The new CRISPR/Cas9 technology was used to powerfully suppress or activate the target gene. The operation makes this technology useful in biology and clinical research [15]. Using this technology, we obtained the Mex3c gene-deficient mice and found that Mex3c^{-/-} mice were much weaker than normal mice and Mex3c^{+/-} mice, which had slower weight gain and lower activity after birth. At 1 month of age or after cutting off mouse tails for genotyping, some mice died. Lu et al. reported that Mex3c-deficient mice died due to poor respiration after birth, similar to IGF1-deficient mice [8]. Therefore, in the present study, we decided to use Mex3c^{+/-}

mice instead of Mex3c^{-/-} mice, which had better physiological conditions than homozygotes. The mice could survive to adulthood and met the requirements of reproductive offspring. The Mex-3 protein was discovered during the study of *C. elegans* embryo development in 1996. This protein family has 4 proteins: Mex-3A, Mex-3B, Mex-3C, and Mex-3D. The genes encoding them are located in humans on chromosomes 1, 15, 18, and 19 [16]. Homozygotes and heterozygotes in Mex3c expression-deficient mice established reduced obesity, reduced fat cells, and decreased blood glucose. Lipid concentrations and insulin sensitivity of homozygotes were higher than in heterozygotes, suggesting that a lower Mex3c expression rate reduces the degree of obesity [7]. However, the relationship between Mex3c and energy balance regulation have not been specifically explained. C-FOS is a fast-acting protein, which is rapidly expressed and reaches a peak within 90–120 min after the body is stimulated [17]. Mice in each group were anesthetized 2 h after intraperitoneal injection of drugs, and brain tissue was removed for processing. We found that control mice had low C-FOS expression in all nuclei in the hypothalamus. After

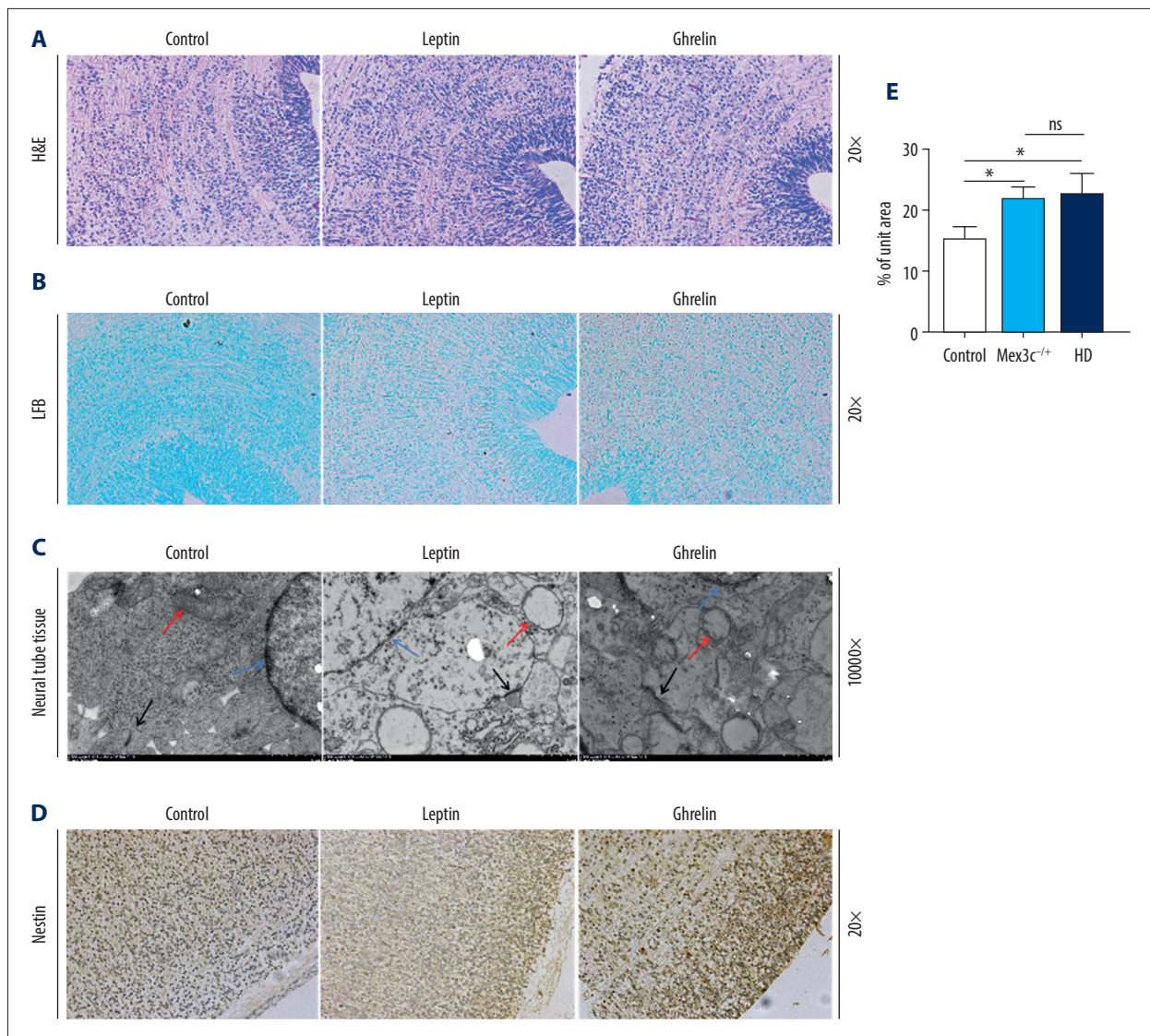


Figure 5. Morphological differences in mouse embryonic neural tube at 14.5 days. **(A)** H&E staining (200 \times). **(B)** LFB staining (200 \times). **(C)** Transmission electron microscopy (TEM) result (10 000 \times). Red arrows represent mitochondria, black arrows represent synapses, blue arrows represent neuron nuclei. **(D)** Nestin expression in each group as determined by immunohistochemistry (200 \times). **(E)** Bar chart of nestin expression (* $P < 0.05$). Scale bar = 100 μ m.

injection of leptin (causing a negative energy balance effect) and ghrelin (causing a positive energy balance effect), the C-FOS expression levels significantly increased ($P < 0.001$). In the study of Mex3c^{+/+} mice, we found that the C-FOS expression in the control group was very high and there was no significant difference from the normal mice after drug intervention ($P > 0.05$). After injection of leptin and ghrelin, it appeared that the C-FOS expression in the leptin intervention group was not significantly different from that in the Mex3c^{+/+} control group ($P > 0.05$), but C-FOS expression in the ghrelin group was significantly reduced. In the DM and PV nuclei, compared with the normal control group, there was no difference in the expression level ($P > 0.05$). C-FOS is a sign of neuronal activation.

Pioneering studies found that C-FOS expression in the hypothalamus nuclei significantly increased after administration of leptin, ghrelin, or other positive and negative energy balance intervention in normal mice [18–20]. We confirmed in the present experiments that leptin and ghrelin were the first messengers to transmit signals to the second messenger of hypothalamic neurons so that the C-FOS expression was the third messenger, causing the specific response of the target cell to function. C-FOS mRNA is a potential Mex3c target mRNA. Mex3c protein can regulate C-FOS mRNA by promoting its nuclear output [21]. Our experimental results show that mice with normal metabolic levels can express their C-FOS. After intervention with positive and negative energy balance,

C-FOS expression was significantly increased. The C-FOS expression level in Mex3c^{-/-} mice (in a state of negative energy metabolism) was high without intervention, and the C-FOS expression did not increase after leptin administration. The expression of C-FOS decreased after ghrelin was administered. These conclusions showed that Mex3c protein participates in the process of body energy balance regulation, which might be achieved by inducing C-FOS expression in the hypothalamus.

The generation of neural tubes is a major event in the development of all animals, and is closely related to subsequent generation of the central and peripheral nervous systems. During neural tube development, the neural plate must be correctly closed accurately to form the neural tube. Otani and Kappen et al. found that during pregnancy of diabetic and hyperglycemic mice, the embryos were not closed at E10.5 days, but the neural tubes of mice of the same strain without diabetes were completely closed at this time [22]. Also, the neural tube closure time in the avian embryos in a hyperglycemic environment was significantly delayed [23]. Disturbances in maternal nutrition and metabolism have significant effects on the development of neural tubes in offspring. Numerous studies confirmed that supplementation with folic acid during pregnancy can significantly reduce the risk of NTDs [24,25]. We chose to use E14.5-day mouse embryos as the in the present study. Compared with mouse embryos in the normal group, the high-fat-diet group and Mex3c mouse embryos not only had difficult pregnancy, but also had fewer offspring. There were different numbers of stillbirths and absorption fetuses, but no neural tube-malformed embryos were observed. Observing the surviving mice in each group, there were no obvious differences in appearance in the 3 groups of mouse embryos. Regularly arranged neurons were seen in pathological sections, and nerve fibers were obvious. The myelin sheath is made of sphingomyelin, which is a tubular sheath wrapped around an axon. LFB staining is a commonly used and reliable staining method for

myelin sheaths [26,27]. When the myelin sheath of immature mice is immature, the sensitivity to LFB staining is higher. LFB staining showed that the normal group was significantly darker, possibly because the degree of myelin sheath development was different between the groups. TEM showed that mitochondria and synapses in the microsystem were impaired or functionally impaired in the HD and Mex3c^{-/-} groups. Nestin is encoded by the nestin gene, which is a unique marker of neural stem cells. Nestin begins to be expressed when neural stem cells start to differentiate into neuronal cells. Accompanying the differentiation of neural cells, nestin expression gradually weakens [28]. Immunohistochemistry results showed that the highest expression of nestin per unit area in the neural tube was in the Mex3c^{-/-} group and the HD group was slightly lower. The normal group had a significantly lower expression percentage than the other 2 groups ($P < 0.05$). The imbalance in energy metabolism affects the development of neural tubes in female mouse embryos during pregnancy.

Conclusions

We constructed a Mex3c gene-deficient mouse model using CRISPR/Cas9 technology. Through reproduction and gene identification, we obtained genetically stable and heterozygous mice. We found that Mex3c was involved in the process of energy metabolism in the body by increasing C-FOS expression in the hypothalamus. In addition, there were some defects in the neural tube of Mex3c^{-/-} female embryos during development, but the specific mechanism is unclear and needs further investigation.

Conflict of interest

None.

References:

1. Hsu PD, Lander ES, Zhang F: Development and applications of CRISPR-Cas9 for genome engineering. *Cell*, 2014; 157(6): 1262–78
2. Sander JD, Joung JK: CRISPR-Cas systems for editing, regulating and targeting genomes. *Nat Biotechnol*, 2014; 32(4): 347–55
3. Hryhorowicz M, Lipiński D, Zeyland J, Słomski R: CRISPR/Cas9 Immune System as a Tool for Genome Engineering. *Arch Immunol Ther Exp (Warsz)*, 2017; 65(3): 233–40
4. Berthoud HR: Multiple neural systems controlling food intake and body weight. *Neurosci Biobehav Rev*, 2002; 26(4): 393–428
5. Greene LA, Tischler AS: Establishment of a noradrenergic clonal line of rat adrenal pheochromocytoma cells which respond to nerve growth factor. *Proc Natl Acad Sci USA*, 1976; 73(7): 2424–28
6. Burrell RA, McClelland SE, Endesfelder D et al: Replication stress links structural and numerical cancer chromosomal instability [published correction appears in *Nature*, 2013; 500(7463): 490]. *Nature*, 2013; 494(7438): 492–96
7. Han C, Jiao Y, Zhao Q, Lu B: Mex3c mutation reduces adiposity partially through increasing physical activity. *J Endocrinol*, 2014; 221(3): 457–68
8. Jiao Y, Bishop CE, Lu B: Mex3c regulates insulin-like growth factor 1 (IGF1) expression and promotes postnatal growth. *Mol Biol Cell*, 2012; 23(8): 1404–13
9. Watts AG, Khan AM, Sanchez-Watts G et al: Activation in neural networks controlling ingestive behaviors: What does it mean, and how do we map and measure it?. *Physiol Behav*, 2006; 89(4): 501–10
10. Kovács KJ: Measurement of immediate-early gene activation – c-fos and beyond. *J Neuroendocrinol*, 2008; 20(6): 665–72
11. Qiu J, Zhang C, Borgquist A et al: Insulin excites anorexigenic proopiomelanocortin neurons via activation of canonical transient receptor potential channels. *Cell Metab*, 2014; 19(4): 682–93
12. Dhillon H, Zigman JM, Ye C et al: Leptin directly activates SF1 neurons in the VMH, and this action by leptin is required for normal body-weight homeostasis. *Neuron*, 2006; 49(2): 191–203
13. Xue J, Gu H, Liu D et al: Mitochondrial dysfunction is implicated in retinoic acid-induced spina bifida aperta in rat fetuses. *Int J Dev Neurosci*, 2018; 68: 39–44

14. Yamaguchi Y, Miyazawa H, Miura M: Neural tube closure and embryonic metabolism. *Congenit Anom (Kyoto)*, 2017; 57(5): 134–37
15. Burstein D, Harrington LB, Strutt SC et al: New CRISPR-Cas systems from uncultivated microbes. *Nature*, 2017; 542(7640): 237–41
16. Buchet-Poyau K, Courchet J, Le Hir H et al: Identification and characterization of human Mex-3 proteins, a novel family of evolutionarily conserved RNA-binding proteins differentially localized to processing bodies. *Nucleic Acids Res*, 2007; 35(4): 1289–300
17. Nestler EJ: Δ FosB: A transcriptional regulator of stress and antidepressant responses. *Eur J Pharmacol*, 2015; 753: 66–72
18. Pedroso JA, Buonfiglio DC, Cardinali LI et al: Inactivation of SOCS3 in leptin receptor-expressing cells protects mice from diet-induced insulin resistance but does not prevent obesity. *Mol Metab*, 2014; 3(6): 608–18
19. Cowley MA, Smart JL, Rubinstein M et al: Leptin activates anorexigenic POMC neurons through a neural network in the arcuate nucleus. *Nature*, 2001; 411(6836): 480–84
20. Okuno H: Regulation and function of immediate-early genes in the brain: Beyond neuronal activity markers. *Neurosci Res*, 2011; 69(3): 175–86
21. Li X, Li Y, Liu C et al: Oocyte-specific expression of mouse MEX3C652AA in the ovary and its potential role in regulating maternal fos mRNA. *Biol Reprod*, 2016; 94(5): 115
22. Otani H, Tanaka O, Tatewaki R et al: Diabetic environment and genetic predisposition as causes of congenital malformations in NOD mouse embryos. *Diabetes*, 1991; 40(10): 1245–50
23. Kappen C: Modeling anterior development in mice: diet as modulator of risk for neural tube defects. *Am J Med Genet C Semin Med Genet*, 2013; 163C(4): 333–56
24. Greene ND, Leung KY, Copp AJ: Inositol, neural tube closure and the prevention of neural tube defects. *Birth Defects Res*, 2017; 109(2): 68–80
25. Miyazawa H, Yamamoto M, Yamaguchi Y, Miura M: Mammalian embryos show metabolic plasticity toward the surrounding environment during neural tube closure. *Genes Cells*, 2018; 23(9): 794–802
26. Khodanovich MY, Sorokina IV, Glazacheva VY et al: Histological validation of fast macromolecular proton fraction mapping as a quantitative myelin imaging method in the cuprizone demyelination model. *Sci Rep*, 2017; 7: 46686
27. Wang C, Sun C, Hu Z et al: Improved neural regeneration with olfactory ensheathing cell inoculated PLGA scaffolds in spinal cord injury adult rats. *Neurosignals*, 2017; 25(1): 1–14
28. Lendahl U, Zimmerman LB, McKay RD: CNS stem cells express a new class of intermediate filament protein. *Cell*, 1990; 60(4): 585–95